

# LCL Filter Design and Performance Analysis for Grid Interconnected Systems

A. Reznik\*, M. Godoy Simões\*, Ahmed Al-Durra\*\*, S. M. Mueen\*\*

\*Colorado School of Mines, EECS Dept., Golden, CO, USA

\*\*Petroleum Institute, Electrical Engineering Department, Abu Dhabi, UAE.

**Abstract**--The use of power converters is very important in maximizing the power transfer from renewable energy sources such as wind, solar, or even a hydrogen-based fuel cell to the utility grid. A LCL filter is often used to interconnect an inverter to the utility grid in order to filter the harmonics produced by the inverter. Even though there is an extensive amount of literature available describing LCL filters, there has been a gap in providing a systematic design methodology. Furthermore, there has been a lack of a state-space mathematical modeling approach that considers practical cases of delta and wye connected capacitors showing their effects on possible grounding alternatives. This paper describes a design methodology of a LCL filter for grid-interconnected inverters along with a comprehensive study of how to mitigate harmonics. The procedures and techniques described in this paper may be used in small-scale renewable energy conversion systems and may also be retrofitted for medium and large-scale grid connected systems.

**Index Terms**--filter; harmonics; inverter; power quality; pulse width-modulated (PWM) inverters;

## I. INTRODUCTION

Voltage source inverters (VSI) are used for energy conversion from a DC source to an AC output, both in a stand-alone mode or when connected to the utility grid. A filter is required between a VSI and the grid, imposing a current-like performance for feedback control and reducing harmonics of the output current. A simple series inductor can be used, but the harmonic attenuation is not very pronounced. In addition, a high voltage drop is produced and the inductor required in the design is very bulky [1].

Commonly a high-order LCL filter has been used in place of the conventional L-filter for smoothing the output currents from a VSI [1], [2]. The LCL filter achieves a higher attenuation along with cost savings, given the overall weight and size reduction of the components. LCL filters have been used in grid-connected inverters and pulse-width modulated active rectifiers [1]-[3], because they minimize the amount of current distortion injected into the utility grid [4]. Good performance can be obtained in the range of power levels up to hundreds of kW, with the use of small values of inductors and capacitors [3]. The higher harmonic attenuation of the LCL filter allows the use of lower switching frequencies to meet harmonic constraints as defined by standards such as,

IEEE-519 and IEEE-1547 [5], [6]. However, it has been observed that there is very little information available describing the systematic design of LCL filters. In order to design an effective LCL filter it is necessary to have appropriate mathematical model of the filter. In this paper, the output filter modeling, filter-designing procedures, and considerations of the passive damping requirements will be thoroughly discussed.

The objective of this paper is to conduct a comprehensive analysis and modeling of the three-phase LCL filter for non-galvanic isolated inverters, suitable for wind energy or photovoltaic applications. Two configurations of three-phase full-bridge dc/ac inverter are compared; first a set of wye-connected filter capacitors with damping, and second a delta-connected filter output connection.

## II. SYSTEM MODELING

### A. Per-Phase Equivalent Modeling of a LCL Filter

The following per-phase equivalent model has been fully described in an earlier paper written by the authors [7]. The LCL filter model is shown in Fig.1, where  $L_1$  is the inverter-side inductor,  $L_2$  is the grid-side inductor,  $C_f$  is a capacitor with a series  $R_f$  damping resistor,  $R_1$  and  $R_2$  are inductors resistances, voltages  $v_i$  and  $v_g$  are the input and output (inverter voltage and output system voltage). A functional block diagram for the grid connected inverter using this LCL filter is shown in Fig.2.

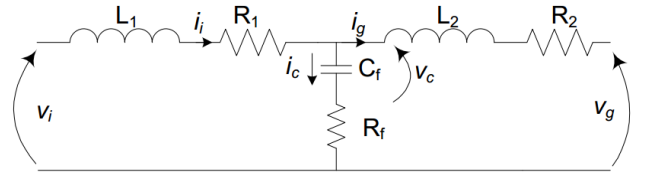


**Fig. 1** LCL filter per phase model.

Currents  $i_i$ ,  $i_c$ ,  $i_g$  are inverter output current, capacitor current, and grid current, respectively. The discussion begins with a brief summary of the two possible configurations for the LCL filter.

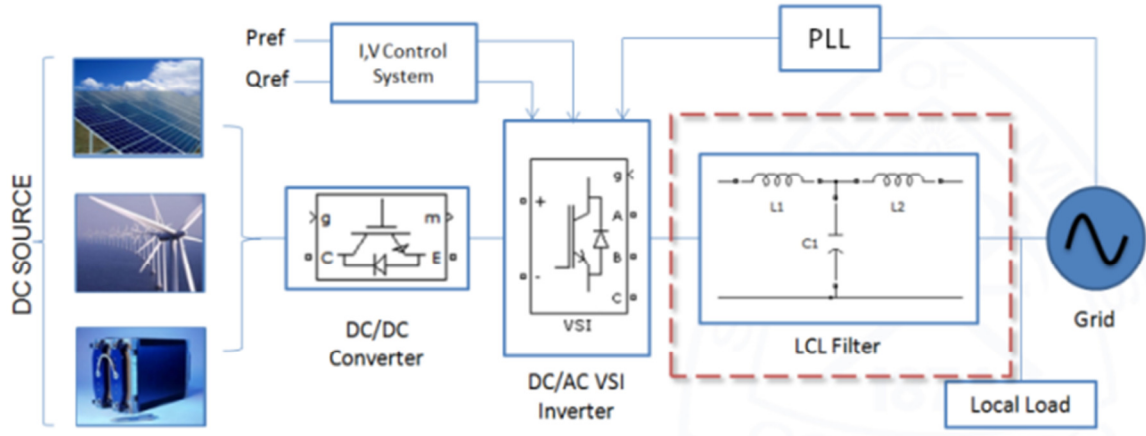


Fig. 2 General schematic for grid interconnected DC power source.

### B. Wye Connected Capacitors

The LCL filter state space model with wye connected capacitors is derived from the per-phase model shown in Fig.2

$$\begin{cases} \frac{dv_c}{dt} = \frac{i_i - i_g}{C_f} \\ \frac{di_i}{dt} = \frac{1}{L_1} (v_i - v_c - R_f(i_i - i_g) - R_1 i_i) \\ \frac{di_g}{dt} = \frac{1}{L_2} (v_c + R_f(i_i - i_g) - v_g - R_2 i_g) \end{cases} \quad (1)$$

The equations show no cross-coupling terms as indicated by the matrix expression (2):

$$\begin{bmatrix} \frac{di_i}{dt} \\ \frac{di_g}{dt} \\ \frac{dv_c}{dt} \end{bmatrix} = \begin{bmatrix} -\frac{R_1 + R_f}{L_1} & \frac{R_f}{L_1} & -\frac{1}{L_1} \\ \frac{R_f}{L_2} & -\frac{R_2 + R_f}{L_2} & \frac{1}{L_2} \\ \frac{1}{C_f} & -\frac{1}{C_f} & 0 \end{bmatrix} \begin{bmatrix} i_i \\ i_g \\ v_c \end{bmatrix} + \begin{bmatrix} \frac{1}{L_1} & 0 \\ 0 & -\frac{1}{L_2} \\ 0 & 0 \end{bmatrix} \begin{bmatrix} v_i \\ v_g \end{bmatrix} \quad (2)$$

$$\dot{x} = Ax + Bu \quad (3)$$

### C. Delta Connected Capacitors

A LCL filter with delta connected capacitors can be analyzed in the  $abc$  stationary frame with the circuit in Fig.3. The voltages and currents can be formulated as given by equations (4) and (5).

$$v_{AB} + v_{BC} + v_{CA} = 0 \quad (4)$$

$$\frac{dv_{AB}}{dt} = \frac{1}{3C_f} i_{iAB} - \frac{1}{3C_f} i_{gAB}$$

where  $i_{iAB} = i_{iA} - i_{iB}$  and  $i_{gAB} = i_{gA} - i_{gB}$ .

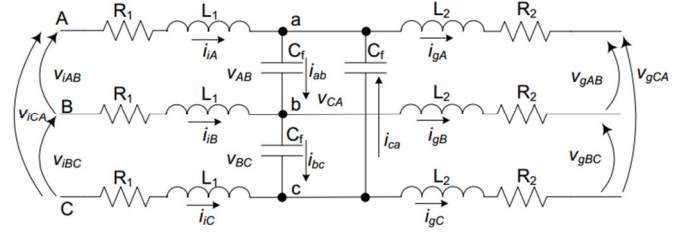


Fig. 3 LCL Filter with delta connected capacitors.

Equation (4) indicates that line-line voltages sum to zero, while the load side equations are given by (6) - (7) with the final formulation in (8).

$$\frac{di_{iAB}}{dt} = -\frac{V_{AB}}{L_1} + \frac{V_{iAB}}{L_1} - \frac{i_{iAB} R_1}{L_1} \quad (6)$$

$$\frac{di_{gAB}}{dt} = -\frac{R_2}{L_2} i_{gAB} + \frac{1}{L_2} V_{AB} - \frac{1}{L_2} V_{gAB} \quad (7)$$

$$\begin{cases} \frac{dv_c}{dt} = \frac{1}{3C_f} i_i - \frac{1}{3C_f} i_g \\ \frac{di_i}{dt} = \frac{1}{L_1} (v_i - v_c - R_f(i_i - i_g) - R_1 i_i) \\ \frac{di_g}{dt} = \frac{1}{L_2} (v_c + R_f(i_i - i_g) - v_g - R_2 i_g) \end{cases} \quad (8)$$

where  $v_c = [V_{AB} V_{BC} V_{CA}]^T$ ,  $i_i = [i_{iAB} i_{iBC} i_{iCA}]^T$ ,  $v_i = [V_{iAB} V_{iBC} V_{iCA}]^T$ ,  $i_g = [i_{gAB} i_{gBC} i_{gCA}]^T$ .

The model used as a continuous state-space plant is given by the matrices  $A$ ,  $B$ ,  $u$  and  $X$  below:

$$\text{where } A = \begin{bmatrix} 0_{3 \times 3} & \frac{1}{3C_f} I_{3 \times 3} & -\frac{1}{3C_f} I_{3 \times 3} \\ -\frac{1}{L_1} I_{3 \times 3} & -\frac{R_1 + R_f}{L_1} I_{3 \times 3} & \frac{R_f}{L_1} I_{3 \times 3} \\ \frac{1}{L_2} I_{3 \times 3} & 0_{3 \times 3} & -\frac{R_2}{L_2} I_{3 \times 3} \end{bmatrix}_{9 \times 9}, \quad (5)$$

$$B = \begin{bmatrix} 0_{3 \times 3} \\ \frac{1}{L_1} I_{3 \times 3} \\ -\frac{1}{L_2} I_{3 \times 3} \end{bmatrix}_{9 \times 3}, \quad u = \begin{bmatrix} V_i \\ V_g \end{bmatrix}_{9 \times 1}, \quad X = \begin{bmatrix} V_c \\ I_i \\ I_g \end{bmatrix}_{9 \times 1}$$

### D. LCL Frequency Response

An important transfer function is  $H_{LCL} = \frac{i_g}{v_i}$ , where the grid voltage is assumed to be an ideal voltage source capable of dumping all the harmonic frequencies. If one sets  $v_g = 0$ , i.e. conditions for current-controlled inverters, the transfer function of LCL filter (neglecting damping) is:

$$H_{LCL}(s) = \frac{1}{L_1 C_f L_2 s^3 + (L_1 + L_2)s} \quad (9)$$

and with some simple algebraic manipulations the transfer function with damping resistance becomes:

$$Hd_{LCL}(s) = \frac{C_f R_f s + 1}{L_1 C_f L_2 s^3 + C_f (L_1 + L_2) R_f s^2 + (L_1 + L_2)s} \quad (10)$$

The Bode plots of the LCL filter without and with damping are shown in Fig.4. The insertion of a series resistance with the capacitor eliminates the gain spike, smoothing the overall response and rolling-off to -180 degrees for high frequency, instead of -270 degrees. It is possible to observe in this Bode diagram, that the closed loop bandwidth must be within 1000 Hz where the phase shift is around -90 degrees.

## III. FILTER DESIGN PROCEDURE

### A. Systematic Filter Design

Several characteristics must be considered in designing a LCL filter, such as current ripple, filter size and switching ripple attenuation. The reactive power requirements may cause a resonance of the capacitor interacting with the grid. Therefore, passive or active damping must be added by including a resistor in series with the capacitor. In this work, the passive damping solution has been adopted, but active solutions can also be applied [1].

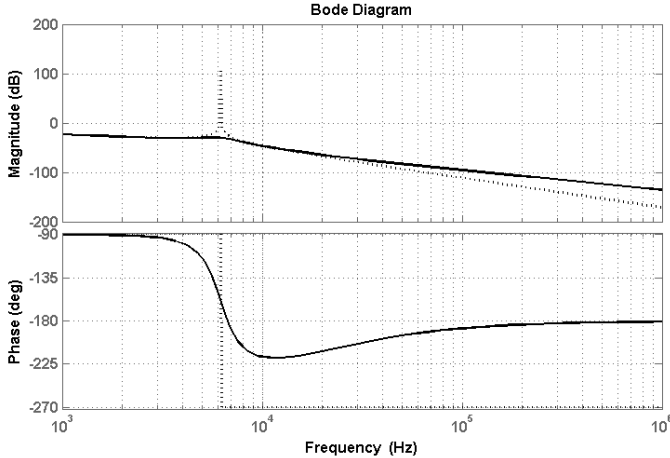


Fig. 4 Bode diagram for damped and undamped cases.

The algorithm for designing the LCL filter is indicated in Fig.5. In the example below, the filter design steps are described in detail.

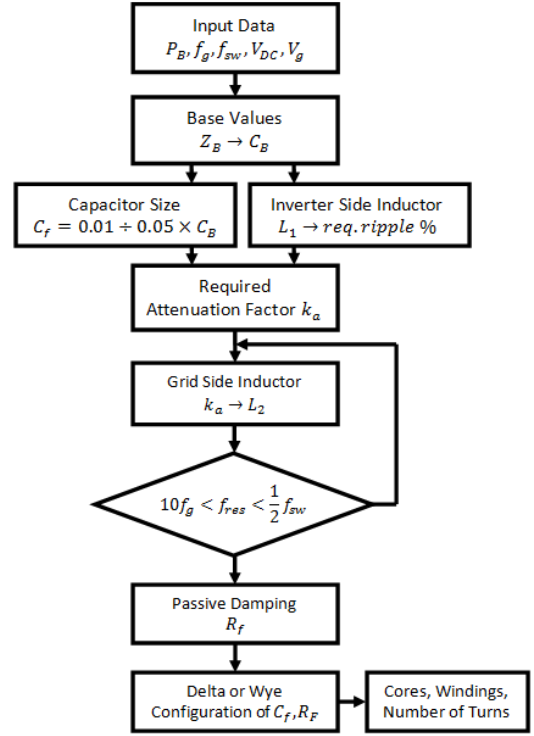


Fig. 5 LCL filter design algorithm.

The following parameters are needed for the filter design:  $V_{LL}$ -line to line RMS voltage (inverter output),  $V_{ph}$ -phase voltage (inverter output),  $P_n$  - rated active power,  $V_{DC}$  -DC-link voltage,  $f_g$ -grid frequency,  $f_{sw}$ -switching frequency,  $f_{res}$ -resonance frequency.

The base impedance and base capacitance are defined by (11) and (12). Thus, the filter values will be referred to in a percentage of the base values:

$$Z_b = \frac{E_n^2}{P_n} \quad (11)$$

$$C_b = \frac{1}{\omega_g Z_b} \quad (12)$$

For the design of the filter capacitance, it is considered that the maximum power factor variation seen by the grid is 5%, indicating that the base impedance of the system is adjusted as follows:  $C_f = 0.05 C_b$ . A design factor higher than 5% can be used, when it is necessary to compensate the inductive reactance of the filter. The maximum current ripple at the output of DC/AC inverter is given by [8]:

$$\Delta I_{Lmax} = \frac{2V_{DC}}{3L_1} (1 - m) m T_{sw} \quad (13)$$

where,  $m$  is the inverter modulation factor (for a typical SPWM inverter).

It can be observed that maximum peak to peak current ripple happens at  $m = 0.5$ , then

$$\Delta I_{Lmax} = \frac{V_{DC}}{6f_{sw} L_1} \quad (14)$$

where  $L_1$  is the inverter side inductor. A 10% ripple of the rated current for the design parameters is given by:

$$\Delta I_{Lmax} = 0.1 I_{max} \quad (15)$$

where

$$I_{max} = \frac{P_n \sqrt{2}}{3 V_{ph}} \quad (16)$$

$$L_1 = \frac{V_{DC}}{6 f_{sw} \Delta I_{Lmax}} \quad (17)$$

The LCL filter should reduce the expected current ripple to 20%, resulting in a ripple value of 2% of the output current [2], [5]. In order to calculate the ripple reduction, the LCL filter equivalent circuit is initially analyzed considering the inverter as a current source for each harmonic frequency in accordance with Fig. 1.

Equations (18) and (19) relate the harmonic current generated by the inverter with the one injected in the grid:

$$\frac{i_g(h)}{i_l(h)} = \frac{1}{|1+r[1-L_1 C_b \omega_{sw}^2 x]|} = k_a \quad (18)$$

or

$$L_2 = \frac{\sqrt{\frac{1}{k_a^2} + 1}}{C_f \omega_{sw}^2} \quad (19)$$

where,  $k_a$  is the desired attenuation.  $C_f = 0.01 \div 0.05 C_b$ .

The constant  $r$  is the ratio between the inductance at the inverter side and the one at the grid side:

$$L_2 = r L_1 \quad (20)$$

Plotting the results for several values of  $r$  helps in evaluating the transfer function of the filter at a particular resonant frequency, depending on the nominal grid impedance [4]. A resistor in series ( $R_f$ ) with the capacitor attenuates part of the ripple on the switching frequency in order to avoid the resonance. The value of this resistor should be one third of the impedance of the filter capacitor at the resonant frequency [9] and the resistor in series with the filter capacitance is given by (23).

$$\omega_{res} = \sqrt{\frac{L_1 + L_2}{L_1 L_2 C_f}} \quad (21)$$

$$10 f_g < f_{res} < 0.5 f_{sw} \quad (22)$$

The resonant frequency range must be considered to satisfy (22)

$$R_f = \frac{1}{3 \omega_{res} C_f} \quad (23)$$

#### IV. LCL FILTER DESIGN EXAMPLE

This section shows a step-by-step procedure used to design a wye capacitor configuration. The specifications are:  $E_n = 120\sqrt{3} V$  - line to line RMS voltage,  $P_B = P_n = 5 kW$  - rated active power,  $V_{DC} = 400 V$  - DC-link voltage,  $\omega_g = 2\pi 60$  - grid angular frequency,  $\omega_{sw} = 15 kHz$  - switching frequency,  $x = 0.05$  - maximum power factor variation seen by the grid,  $k_a = 0.2$  (20%) - attenuation factor. Therefore, the base impedance and the base capacitance are  $Z_B = 8.64 \Omega$ ,  $C_B = 307 \mu F$  respectively (parameters are shown in Table I).

1. Using 10% allowed ripple equation (15) gives an inductance  $L_1 = 2.23 mH$
2. The maximum capacitor value is  $16.63 \mu F$  in order to be within the limit of 5% of the base value of  $C_B$ . After rounding to the closest commercial value,  $C_f = 15 \mu F$  for the wye configuration or  $5 \mu F$  for the delta connection.
3. One can set the desired attenuation  $k_a = 20\%$  and then using (19)  $L_2$  is found to be  $0.045 mH$ .
4. Putting all calculated parameters of  $L_1$ ,  $C_f$  and  $L_2$  into (21), gives  $f_{res} = 6450 kHz$  which meets condition from (22).
5. Equation (23) gives the damping resistance  $R_f = 0.55 \Omega$  for wye configuration or  $1.65 \Omega$  for delta connection.
6. The construction of the inductors was defined using the software available on web site of the Magnetics® Company [10] and presented in Table II.
7. The inductor parameters were validated during the experimental setup by taking note of the inductors values when measuring voltage, current and times with an oscilloscope and computing  $L = (\frac{\Delta t}{\Delta i}) / V$ .

TABLE I  
TESTED SYSTEM PARAMETERS

$f_g$	Grid frequency	60Hz
$f_{sw}$	PWM carrier frequency	15kHz
$P_n$	Nominal Power	5kW
$V_g$	Phase grid voltage	120V
$V_{DC}$	DC link Voltage	400V
$L_1$	Inverter side inductor	2.33mH
$L_2$	Grid side inductor	0.045mH
$C_f$	Capacitor filter Y/ $\Delta$	15 $\mu F$ /5 $\mu F$
$R_f$	Damping Resistor Y/ $\Delta$	0.55 $\Omega$ /1.65 $\Omega$

TABLE II  
INDUCTORS PARAMETERS

Parameter	$L_1$	$L_2$
Inductance(mH)	2.33mH	0.045mH
Core Type	77102-A7	77258-A7
Number in Stack	5	1
Wire	AWG 12	AWG 12
Number of Turns	116	43

#### V. SIMULATION RESULTS AND ANALYSIS

##### A. System Modeling

Two models for LCL filter evaluation have been analyzed using Matlab® and Simulink® Power System ToolBox

simulation environment as shown in Fig.6 and Fig.7, the same simulation structure has been implemented in the hardware. The sampling time and simulation step-size is  $0.5\mu\text{s}$ , whereas the sampling time for the control system is  $100\mu\text{s}$ . Such a choice of multi-sampling is done in order to allow the

hardware implementation using a Hardware-In-the-Loop dSPACE 1104 system [11]. Both voltage and current control systems for stand-alone and grid-connected mode are developed using Park and Clarke transformations with PI control in the  $dq$  frame.

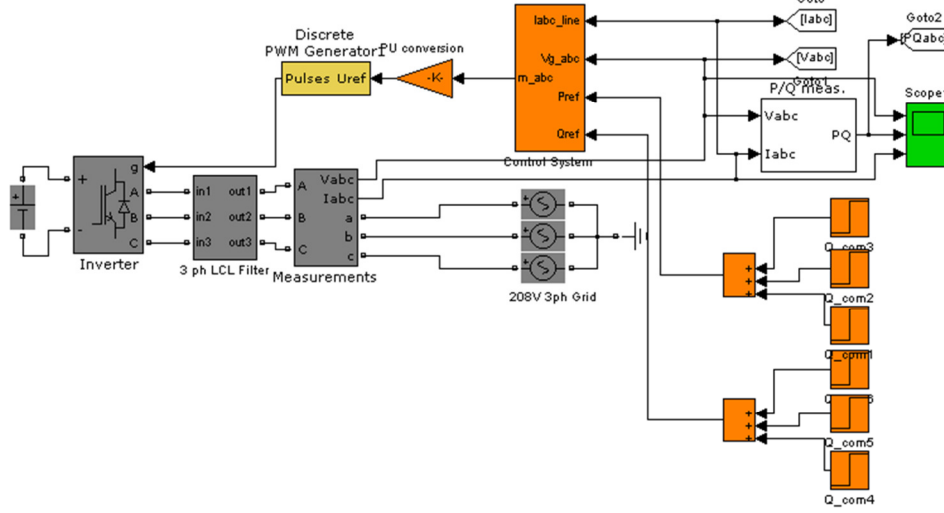


Fig. 6 Grid connected inverter.

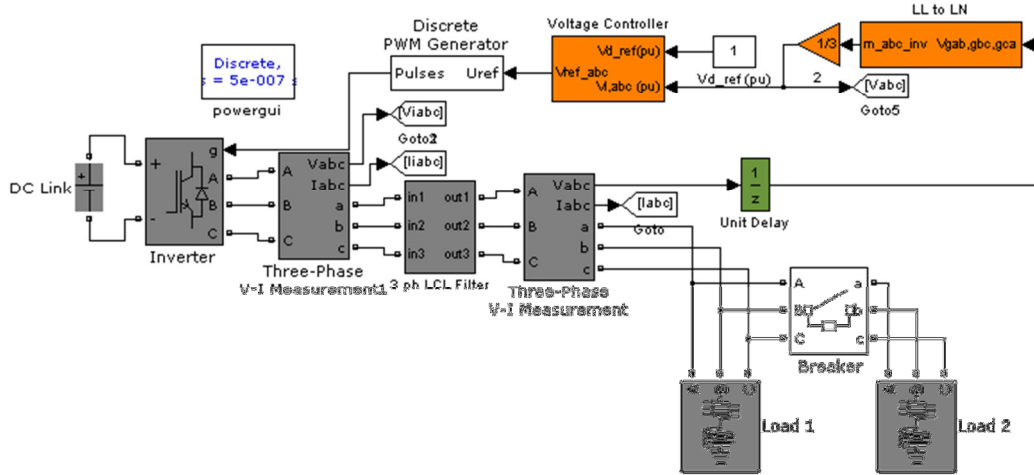


Fig. 7 Stand-alone inverter.

## VI. EXPERIMENTAL DATA AND PERFORMANCE ANALYSIS

The proposed LCL filter has been validated using a grid-connected three-phase 5 kW inverter prototype with the ability to operate in a stand-alone mode. The LCL filter shown in Figures 8 and 9, based on parameter values listed in Table I, Table II and Table IV, has been designed and built. The control algorithm was executed in a dSPACE 1104 real-time platform. Two types of magnetic cores from Magnetics (www.mag-inc.com) and software [12] were used in the assembly of the inductors.

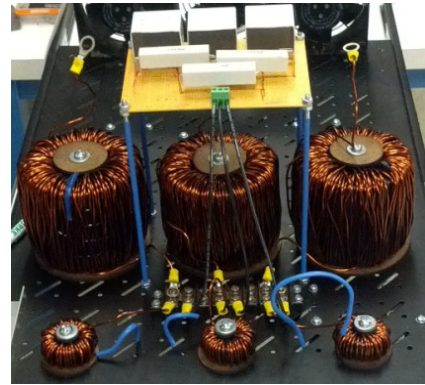


Fig. 8 Implemented LCL filter.



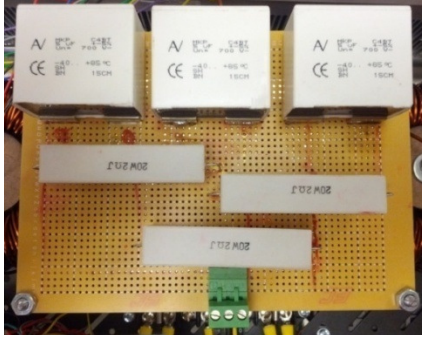


Fig. 9  $C_f, R_f$  delta circuit.

The *Inductor Design* software assisted in selecting the optimum core for inductor applications. This software uses an algorithm intended to specify the smallest design package size for the given input parameters (current, inductance value, frequency).

The LCL filter was then verified by experimental results. Fig. 10 through Fig. 12 shows important system variables, captured with an Agilent MSO-X 3104A oscilloscope. The first set of experimental results obtained is shown in Fig. 10 and Fig. 11, during which the proposed installation is supplying 100% nominal load power in open-loop voltage control mode. A SPWM strategy is used in the inverter and the DC link voltage is kept at 400 V. The output inverter phase-voltage output can be seen in Fig.10 (before the filter), the THD is 44%. As it can be seen on Fig.11 the voltage output from LCL filter is smooth and harmonic analysis show the effectiveness of the designed filter. The attenuation has been specified for maximum 2% THD. In practice the actual value of voltage and current THD is even less than 2%. Fig.12 shows the current flowing in filter capacitor, which dissipated in the damping resistor.

TABLE IV  
ACTUAL FILTER PARAMETERS

$L_1$	Inverter side inductor	2.33mH Custom design
$L_2$	Grid side inductor	0.045mH Custom design
$C_f$	Capacitor filter, $\Delta$	MKP C4BT, 700 VAC, 5 $\mu$ F
$R_f$	Damping Resistor, $\Delta$	Sand Stone, 2 $\Omega$ , 20W

Fig.13 shows the measurements captured by a Power Quality Analyzer Fluke 43B. Fig.13 (a) represents the single phase measurements of voltage, current and power. In this situation the inverter provides 1.2 kW power to the load under nominal voltage and frequency conditions. The THD in this case, seen on Fig.13 (b) is 0.3%. Various tests have been conducted in stand-alone mode for load with different power factors, in all cases the filter output voltage has THD less than 2%.

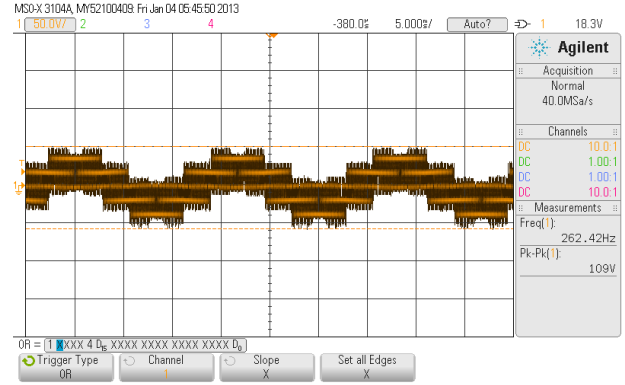


Fig. 10 Inverter output voltage.

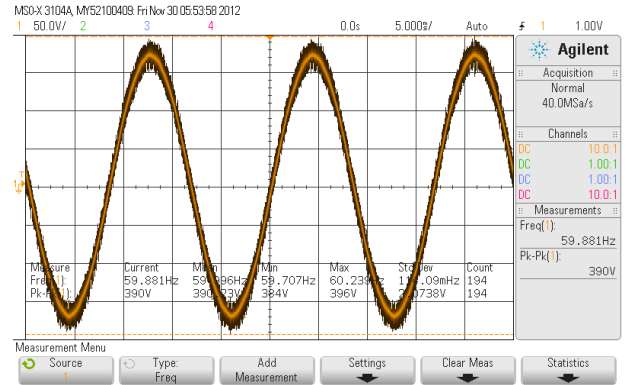


Fig.11 Output voltage (after the LCL filter).

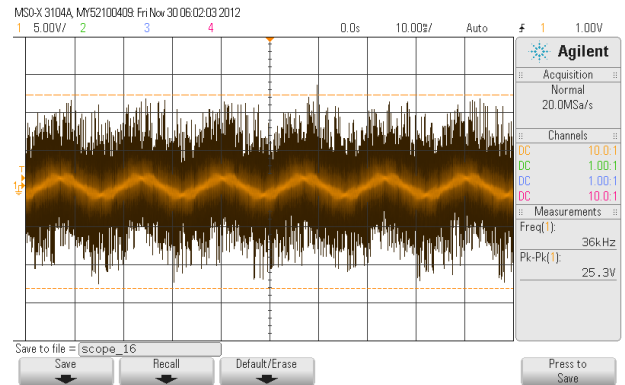


Fig.12 Capacitor current.

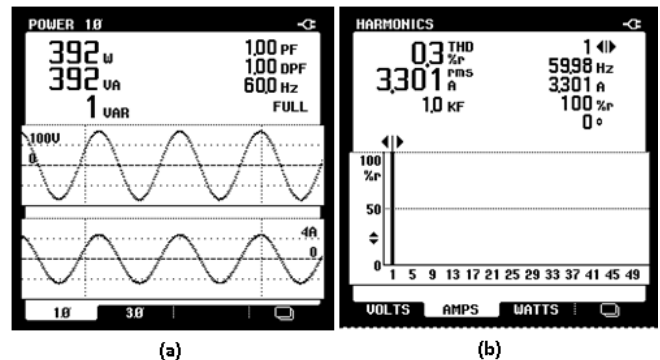
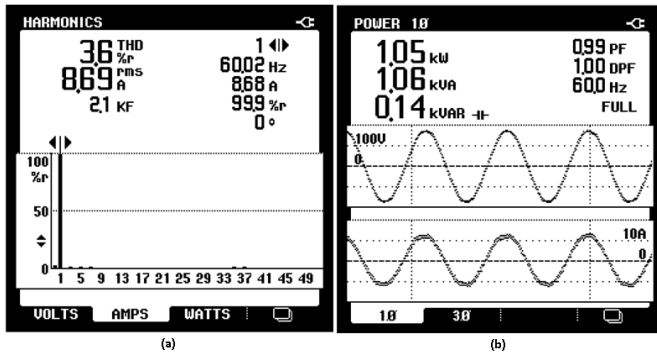


Fig.13 THD analysis and experimental data for stand-alone mode.

The LCL filter has also been tested in a grid connected mode, in order to show the performance under a current control loop. The phase voltage, line current and power factor (PF=0.99) are shown in Fig. 14 (a) and (b). In this case the inverter provides 3 kW (1.05 kW for a per-phase measurement) to the grid. The THD of injected current is 3.6% as seen in Fig. 14 (a). It can be observed that the THD of injected current is higher in grid-connected mode, but still less than required specification of 5%.



**Fig.14** THD analysis and experimental data for grid connected mode (PF=0.99).

The phase voltage, line current and power with PF=0.94 lag injected to the grid are shown on Fig. 15 (a) and (b). In this case the inverter provides 3 kW (1.06 kW per-phase measurement) and 1.2 kVar (390 Var per-phase measurement) to the grid. The THD of injected current is 3.3%.

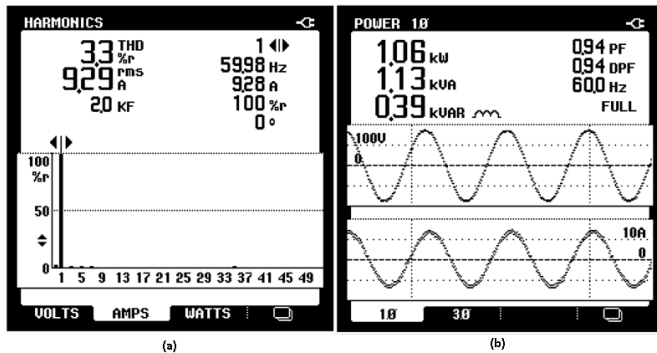


**Fig.15** THD analysis and experimental data for grid connected mode (PF=0.94 lag).

## VII. CONCLUSION

This paper proposes a systematic LCL filter design methodology for grid-interconnected inverter systems. The LCL filter reduces the switching frequency ripple and helps in coupling with a current-like performance to the utility grid. The paper describes a comprehensive and detailed design procedure for the LCL filter. It was found that the proposed design meets industry standards and allows a total harmonic distortion (THD) within a prescribed range. A theoretical design procedure has been fully compared by experimental results. The design approach is also applicable with front-end

inverters used in small and medium-scale distributed dc power sources, such as photovoltaic systems, fuel cells and wind turbine systems (with rectifiers) and can retrofit existing medium and large power systems as well.

## VIII. ACKNOWLEDGMENT

The authors acknowledge the grant given by the Petroleum Institute, Abu Dhabi (UAE) and the Center of Advanced Control of Energy and Power Systems (ACEPS) at Colorado School of Mines. This work has also been partially supported by the US National Science Foundation Award #0931748. The authors gratefully acknowledge Dr. Ravel Ammerman, Colorado School of Mines for his comments and review.

## REFERENCES

- [1] F. Bouchafaa, D. Beriber, and M. S. Boucherit, "Modeling and control of a grid connected PV generation system," in *Control & Automation (MED), 18th Mediterranean Conference*, 2010, pp. 315–320.
- [2] M. Liserre, F. Blaabjerg, and S. Hansen, "Design and Control of an LCL-Filter-Based Three-Phase Active Rectifier," *IEEE Transactions on Industry Applications*, vol. 41, no. 5, pp. 1281–1291, Sep. 2005.
- [3] V. Blasko and V. Kaura, "A Novel Control to Actively Damp Resonance in Input LC Filter of a Three-Phase Voltage Source Converter," *IEEE Transactions on Industry Applications*, vol. 33, no. 2, pp. 542–550, 1997.
- [4] Y. Tang, S. Member, P. C. Loh, P. Wang, and F. H. Choo, "Generalized Design of High Performance Shunt Active Power Filter With Output LCL Filter," *IEEE Transactions on Industrial Electronics*, vol. 59, no. 3, pp. 1443–1452, 2012.
- [5] "519-1992 IEEE Recommended Practices and Requirements for Harmonic Control in Electrical Power Systems," *IEEE Std 519-1992*, 1993.
- [6] "1547.1 IEEE Standard Conformance Test Procedures for Equipment Interconnecting Distributed Resources with Electric Power Systems," *IEEE Std 1547.1-2005*, 2005.
- [7] A. Reznik, M. G. Simões, A. Al-durra, and S. M. Mueen, "LCL Filter Design and Performance Analysis for Small Wind Turbine Systems," in *Power Electronics and Machines in Wind Applications (PEMWA), IEEE*, 2012, pp. 1–7.
- [8] V. H. Prasad, "Average current mode control of a voltage source inverter connected to the grid: Application to different filter cells," Master's Thesis, Dept. Electrical Engineering, Virginia Tech, Blacksburg, Virginia, 1997.
- [9] S. V. Araújo, A. Engler, B. Sahan, V. U. Kassel, F. Luiz, and M. Antunes, "LCL Filter design for grid-connected NPC inverters in offshore wind turbines," in *The 7th International Conference on Power Electronics*, 2007, pp. 1133–1138.
- [10] "Inductor Design | Magnetics®." [Online]. Available: <http://www.mag-inc.com/design/software/inductor-design>. [Accessed: 02-Feb-2013].
- [11] C. da Silva Postiglione and M. G. Simoes, "dSPACE based implementation of a grid connected smart inverter system," in *2010 IEEE 12th Workshop on Control and Modeling for Power Electronics (COMPEL)*, 2010, pp. 1–5.
- [12] "Inductor Design Calculator." [Online]. Available: <http://www2.mag-inc.com/calculators/Inductor-Design-Calculator>. [Accessed: 15-Dec-2012].